Available online at www.sciencedirect.com
SCIENCE DIRECT®
Carbon 44 (2006) 37–45
CARBON
www.elsevier.com/locate/carbon

Carbon nanotube reinforced hydroxyapatite composite coatings produced through laser surface alloying

Y. Chen [a,*], Y.Q. Zhang [b], T.H. Zhang [a], C.H. Gan [a], C.Y. Zheng [a], G. Yu [a]

[a] The State Key Laboratory of Nonlinear Mechanics, Institute of Mechanics, Chinese Academy of Sciences, 15 Beisihuanxi Road, 100080 Beijing, China
[b] Department of Technology and Physics, Zhengzhou University of Light Industrial, 5 Dongfeng Road, 450002 Zhengzhou, China

Received 2 April 2005; accepted 14 July 2005
Available online 31 August 2005

Abstract

Carbon nanotube (CNT) reinforced hydroxyapatite composite coatings have been successfully fabricated by laser surface alloying. The phase compositions and the microstructure of the composite coatings were studied using X-ray diffraction, scanning electron microscopy, transmission electron microscopy (TEM) and high-resolution transmission electron microscopy (HRTEM). TEM observation showed that a large amount of CNTs can be found with their original tubular morphology in the composite coatings, even though some CNTs react with titanium element in the substrate during laser irradiation. Additionally, measurement on the elastic modulus, hardness of the composite coatings by nanoindentation tests indicated that the mechanical properties are affected by the amount of CNTs in the starting precursor materials. Therefore, CNT reinforced hydroxyapatite composite coating is a promising coating material for high-load-bearing metal implants.
© 2005 Elsevier Ltd. All rights reserved.

Keywords: Microstructure; Mechanical properties; Coating

1. Introduction

Carbon nanotubes (CNTs) have been an attractive candidate for fundamental research studies since their discovery by Iijima [1]. Several applications were proposed for CNTs many of which are concerned with conductive or high strength composites [2–4], in which the inclusion of CNTs in a ceramic matrix is expected to produce composites possessing high stiffness and improved mechanical properties compared to the single-phase ceramic material [5]. For example, Lupo et al. [5] successfully fabricated zirconium oxide ZrO_2/carbon nanotube composites by hydrothermal crystallization at 200 °C for 8 h of zirconium hydroxide ($Zr(OH)_{4n}H_2O$; $n = 8$–16) in the presence of carbon nanotubes, and Seeger et al. [6] firstly synthesized multiwalled carbon nanotube/SiO_2 composites by means of partial matrix melting caused by a Nd:YAG laser.

Recently, hydroxyaptite (HA) has received increasing attention as a bone implant material to promote the ability to bond chemically with living bone tissues owing to its similar chemical composition and crystal structure as apatite in the human skeletal system [7]. However, the intrinsic brittleness and poor strength of sintered HA restricts its clinical applications under load-bearing conditions. As a result, one of its major applications is as a covering material for titanium or other metal used in implants [8]. In recent years, lots of investigations have been carried out to fabricate HA coating [8,12] or HA composite coating [9–11] using a plasma spraying technique. Although plasma sprayed HA coatings have successful improvement on promoting bone attachment and integration of the implants [12], the long-term stability of these coatings is still a very challenging issue since these coatings trend to have uncontrollable dissolution and sometimes

* Corresponding author. Tel.: +86 10 62651166; fax: +86 10 62521859.
E-mail address: chenyao27@163.com (Y. Chen).

0008-6223/$ - see front matter © 2005 Elsevier Ltd. All rights reserved.
doi:10.1016/j.carbon.2005.07.011

exhibit insufficient bond strength to the metal substrate [13,14]. Therefore, there are needs for improving further the mechanical properties of these coating materials and the bond strength of HA/metal interface. It is well known that the carbon nanotubes (CNTs) possess excellent mechanical properties and chemical stability resulted from their cylindrical graphitic structure, and carbon is one of known fundamental elements in the development of life on the planet Earth [15]. Therefore, hydroxyapatite composite coatings reinforced with CNTs might have tailored properties including high strength and good bioactivity. Meanwhile, metallurgical bonding between the HA and the metallic substrate can be easily obtained using laser surface processing. Furthermore, the attractions of using nanoindentation techniques to study coated system is that it is good candidate for investigating microplasticity of these coated system locally, in which both the force and the displacement of a small-scale indenter are measured in an extremely sensitive way [16].

To the knowledge of the authors, meager information is available as regards the fabrication and the evaluation of mechanical properties of laser surface alloyed CNT reinforced HA composite coating. In this paper, the aim is to fabricate HA composite coating, in which CNTs as a reinforcement, using laser surface alloying, and evaluate the mechanical properties using nanoindentation.

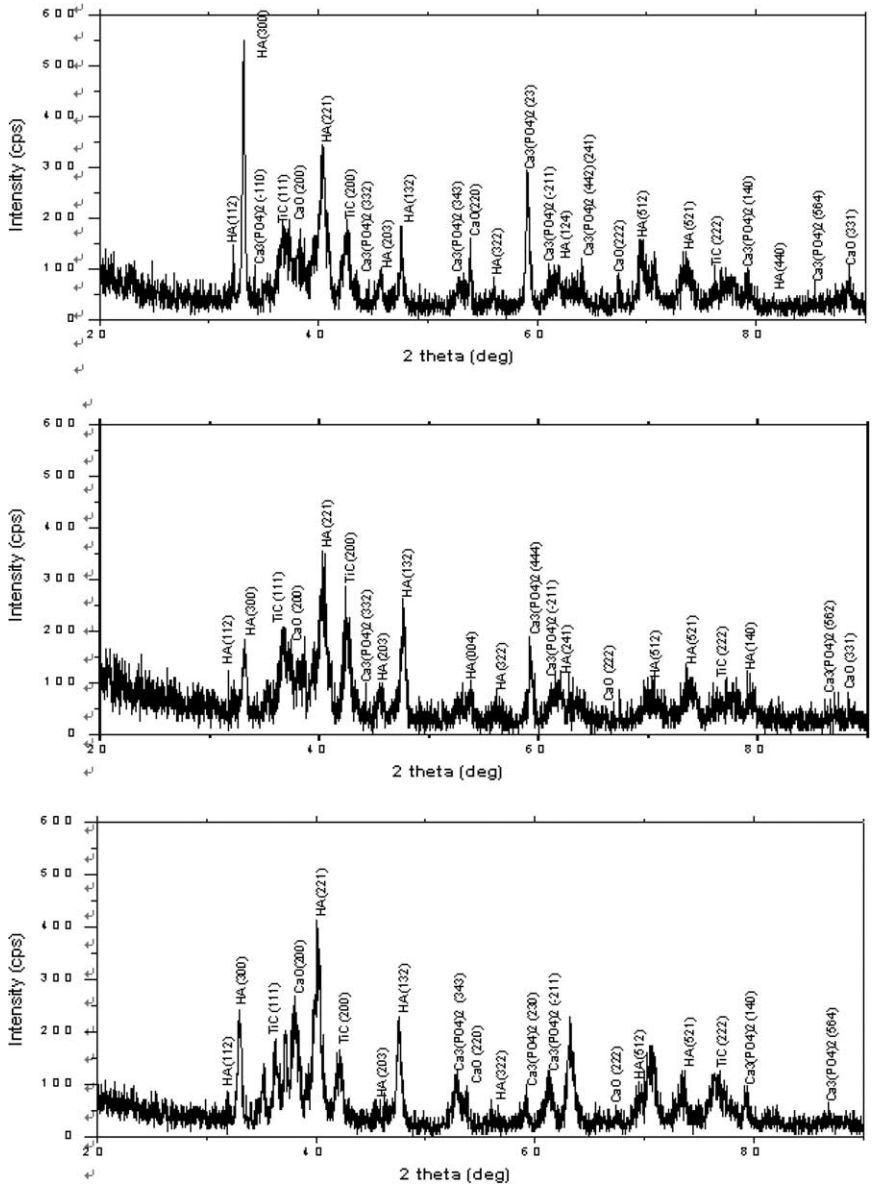

Fig. 1. XRD results of laser surface alloyed CNTs reinforced HA coatings with powder mixtures of HA–5% CNTs (a), HA–10% CNTs (b) and HA–20% CNTs (c), respectively (wt.%).

2. Experimental procedures

Commercially hydroxyapatite powder with an average particle size ranging from 30 to 50 μm and the commercially multiwalled carbon nanotubes (CNTs) with a diameter from 20 to 40 nm and the length from 5 to 15 μm were selected as starting precursor materials for fabricating carbon nanotube (CNT) reinforced hydroxyapatite composite coatings by a laser surface alloying technique. The CNT powder was cleaned in acetone and dehydrated at 473 K before mixing with hydroxyapatite powder. The powder mixtures were mechanically ball-milled together in four different weight proportions, namely 0%, 5%, 10% and 20% CNTs. The substrate used for the coatings was of Ti–6Al–4V with a dimension size of $60 \times 30 \times 5$ mm. Prior to laser surface alloyed composite coatings, the substrates were preheated to reduce the residual thermal stress. The experiments of laser

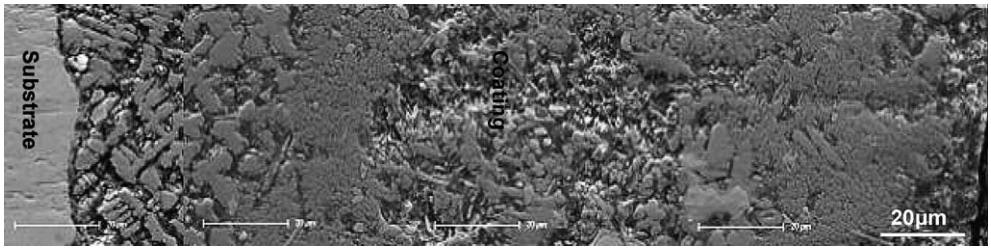

Fig. 2. Field emission SEM images showing the overview microstructure on the cross-section of the laser surface alloyed coating with a powder mixture of HA–10% CNTs (wt.%).

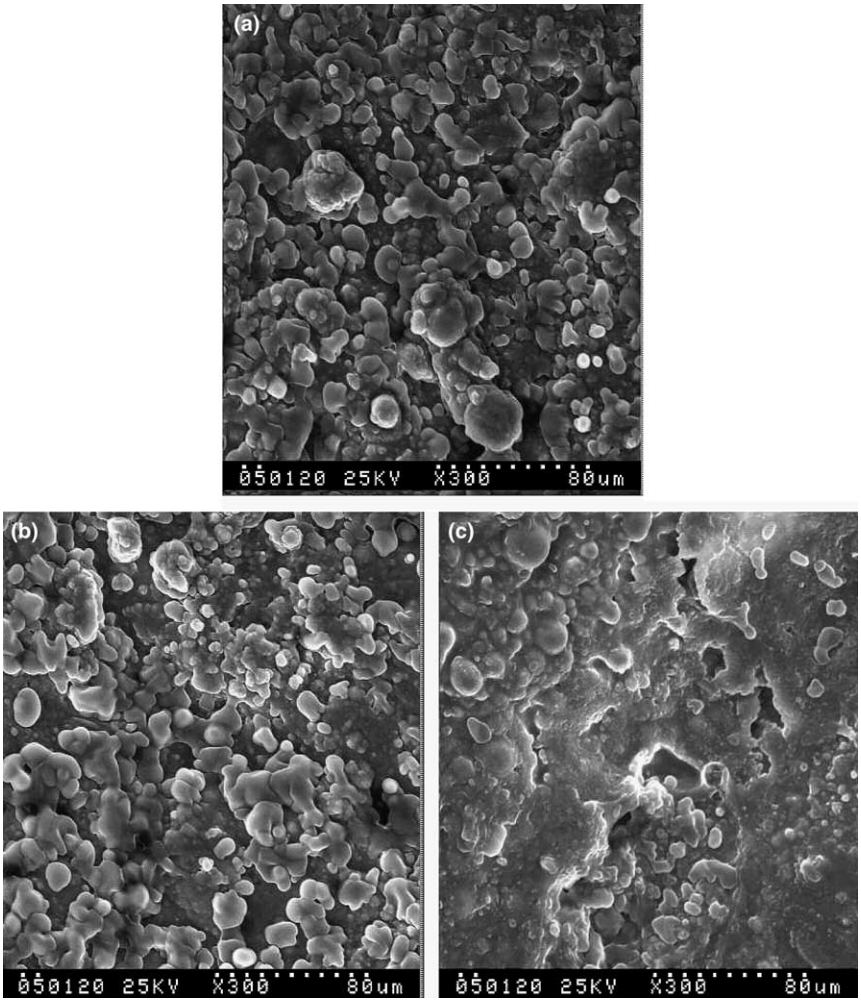

Fig. 3. SEM micrographs showing the surface morphology of as-alloyed with a powder mixtures of HA–5% CNTs (a), HA–10% CNTs (b) and HA–20% CNTs (c).

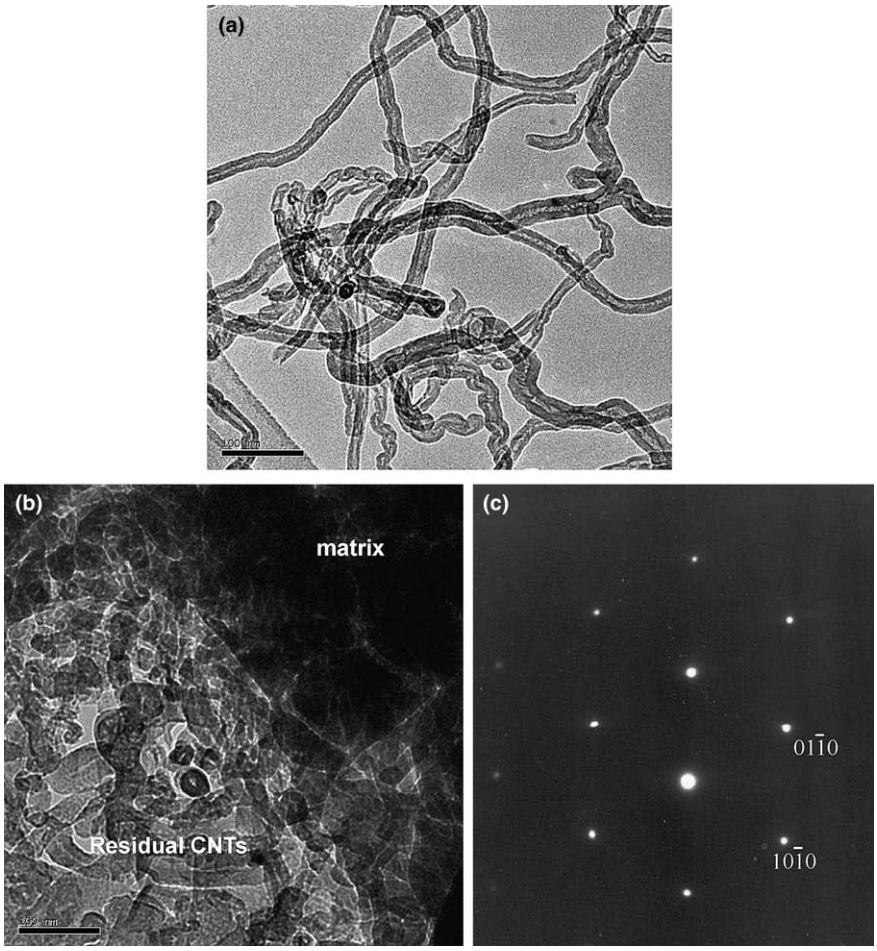

Fig. 4. TEM image showing the typical morphology of as-prepared CNTs (a), residual CNTs in laser surface alloyed coating (b), the selected area diffraction pattern of HA in the direction of [0001] (c).

surface alloying were carried out using a HL2006D Nd:YAG laser, and the laser processing parameters were selected as: laser outpower 400 W, beam diameter 4.0 mm and the beam scanning speed 4 mm/s.

The cross-section of the as-alloyed CNT reinforced HA composite coatings were prepared for the metallographic samples using standard mechanical polishing procedures, thin-foil samples for TEM observation were cut from laser surface alloyed coating, paralleling to the direction of laser beam movement. They were mechanically thinned to 50 μm and then thinned by argon ion milling. Microstructure was characterized using Neophot optical microscopy (OM), SIRION400NC field emission scanning electron microscopy (FEI, Netherlands), transmission electron microscopy (TEM) and high-resolution transmission electron microscopy (HRTEM) in a JEM-2010 operating at 200 kV, respectively. The surface of the coating was coated with gold and morphological observation was employed by using S-570 scanning electron microscopy (SEM). Phase constituents of composite coatings were analyzed by X-ray diffraction (XRD) using a Rigaku D/max 2200 diffractometer with Cu K_α radiation operated at a voltage of 40 kV, a current of 40 mA and a scanning rate of 5° min^{-1}.

Nanoindentation tests were conducted using a MTS Nano Indenter® XP with a Berkovich diamond tip. Hardness and elastic modulus of the coating were measured as a function of indentation depth using a continuous stiffness measurement (CSM) method. The typical nanoindentation test consists of seven subsequent steps: approaching the coating surface; determining the contact point; loading to peak load; holding the tip for 10 s at the peak load; unloading 90% of peak load; holding the tip for 100 s at 10% of the peak load for thermal drift correction; unloading completely. The hardness and elastic modulus were obtained from the curves using Oliver–Pharr method [17]. Indents surface observation was performed by a S-570 scanning electron microscopy (SEM).

3. Results and discussion

XRD results of the laser surface alloyed coatings with the powder mixture of HA–5% CNTs, HA–10% CNTs

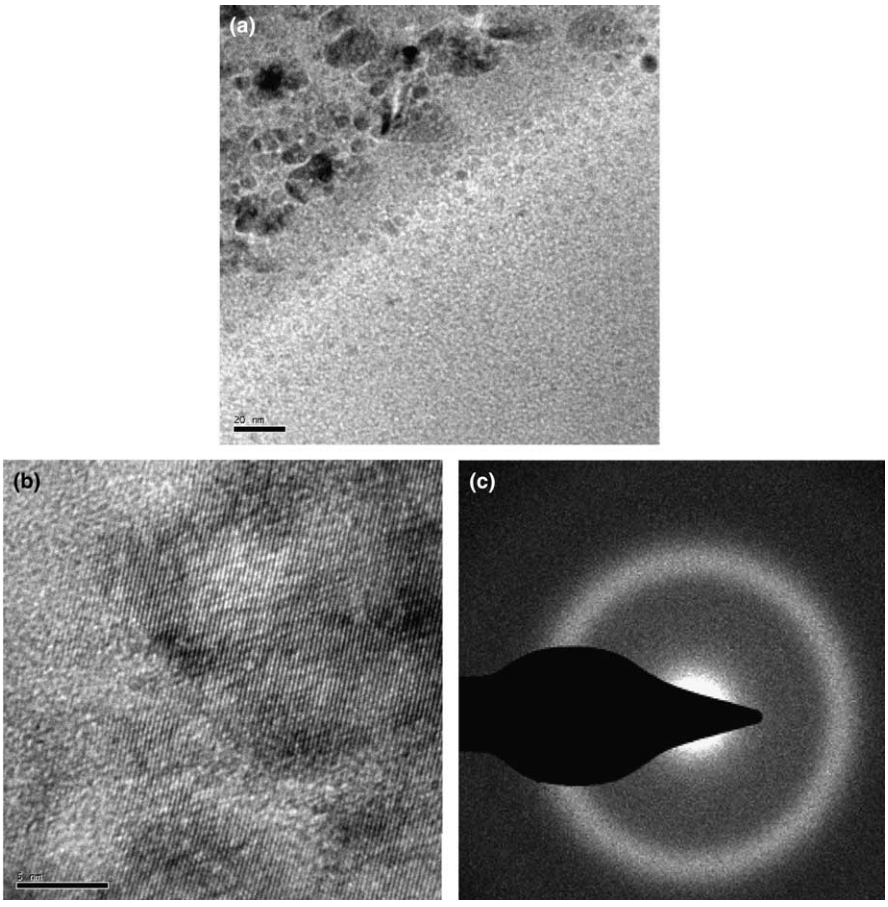

Fig. 5. TEM image showing amorphous regions in conjunction with crystalline HA in the as-alloyed coating (a), corresponding $(30\bar{3}1)$ HRTEM of crystalline HA (b) and the selected area diffraction of the amorphous regions (c).

and HA–20% CNTs, respectively, are presented in Fig. 1. It shows that the constituent phases of the as-alloyed coating are mainly HA, TCP, CaO and TiC. Meanwhile, compared with the relative peak intensity of these XRD patterns, it is clearly seen that the volume fraction of HA decreases and that of TiC increases with increasing of content of CNTs in the powder mixtures. The results imply that the CNTs have reacted partially with Ti, from Ti–6Al–4V substrate, to form TiC, and HA has partially decomposed into CaO and TCP. It is well known that the titanium element has a much larger negative heat of formation (184.0 kJ/mol) with carbon than that of other elements in the laser-generate pool, suggesting that Ti and C have the largest driving force to form TiC. Therefore, the reaction of Ti with C is favored during the laser surface alloying. Also, the temperature of the laser-generated pool is more higher than the melting point of HA (1450 °C), leading to the decomposition of HA to form α-TCP and TTCP. Being an unstable phase at room temperature, α-TCP naturally transform to β-TCP (a stable phase at room temperature) at about 1100 °C [18]. Concerning the TTCP phase, it would further decompose to form HA and CaO [19]. However, no CNTs peaks were found in the XRD patterns of the as-alloyed composite coatings, as shown in Fig. 1, indicating that either the CNTs in the precursor materials have been reacted completed with Ti or a small volume fraction of residual CNTs introduced in the composite coatings is difficult to detect within the sensitivity limit of XRD. Therefore, other

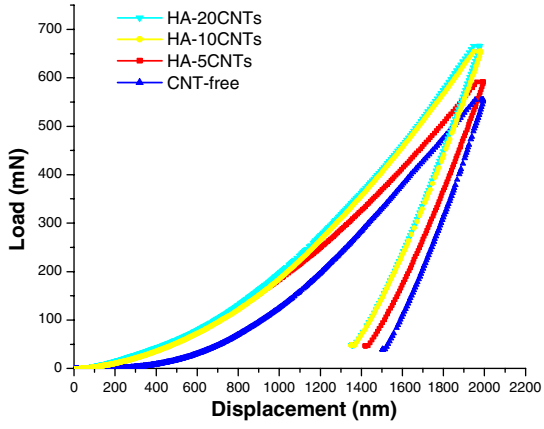

Fig. 6. Typical load–displacement curves of laser surface alloyed coating with different content of CNT.

method is needed to employed to confirm whether the existence of residual CNTs in the composite coatings or not.

It is evident from Fig. 2 that the bonding to the substrate is of high-quality metallurgical fusion bonding, leading to strong bond strength of coating/metal interface. Also, it is clearly seen that the laser surface alloyed coating is relatively dense though some pores can be seen from Fig. 2. SEM micrographs of the surface morphology of the as-alloyed CNT reinforced HA coatings are shown in Fig. 3. Obviously, the coating has a rough surface with little interlinking of pores, which are very helpful to mechanical fixation of the living bone tissues.

TEM observations are conducted to confirm the existence of CNTs in the laser surface alloyed coating, and the images are shown in Fig. 4. Fig. 4(a) shows a typical tubular morphology of as-prepared CNTs. Fig. 4(b) shows the typical morphology of residual CNTs in the as-alloyed coating. It is obvious that some CNTs with their originally tubular structure can be observed after laser surface alloying. It is clearly seen that CNTs still keep their cylindrical graphitic structure due to both the high thermal stability and the high chemical stability of the CNTs [20,21], implying that the introduced CNTs in the as-alloyed composite coatings are expected to maintaining their original excellent mechanical properties. Furthermore, the selected area diffraction pattern in the matrix of the coating shows that the matrix is hydroxyapatite (Fig. 4(c)). According to the above-results, CNTs have been successfully introduced into the HA matrix using laser surface alloying.

In the as-alloyed CNT reinforced HA coatings, amorphous region is also observed, which is in conjunction with these crystalline hydroxyapatite, as shown in Fig. 5(a). Results of high-resolution transmission electron microscopy (HRTEM) for the crystalline hydroxyapatite and selected area diffraction (SAD) for the amorphous region are indicated in Fig. 5(b) and (c), respectively. As is known, laser surface alloying is a rapid heating/rapid cooling process, and therefore the solidification of laser-generated pool is far from the equilibrium solidification, leading to the formation of metastable phase such as amorphous.

In the present work, nanoindentation technique is employed to study the variation of the mechanical properties of laser surface alloyed coatings with different CNT contents, as shown in Fig. 6. It shows that the load increases with increasing content of carbon nanotube in the powder mixtures, indicating that the higher the content of carbon nanotube, the higher the hardness and the elastic modulus. After removal of the indenter tip, the plastic deformation of CNT-free coating is about 1480 nm, while 1290 nm for the HA–20% CNTs coating. This means the CNT-free hydroxyapatite coating undergoes a larger plastic deformation during nanoindentation experiments.

The hardness and elastic modulus curves as a function of indentation depth are shown in Fig. 7, and the average hardness and elastic modulus for these compo-

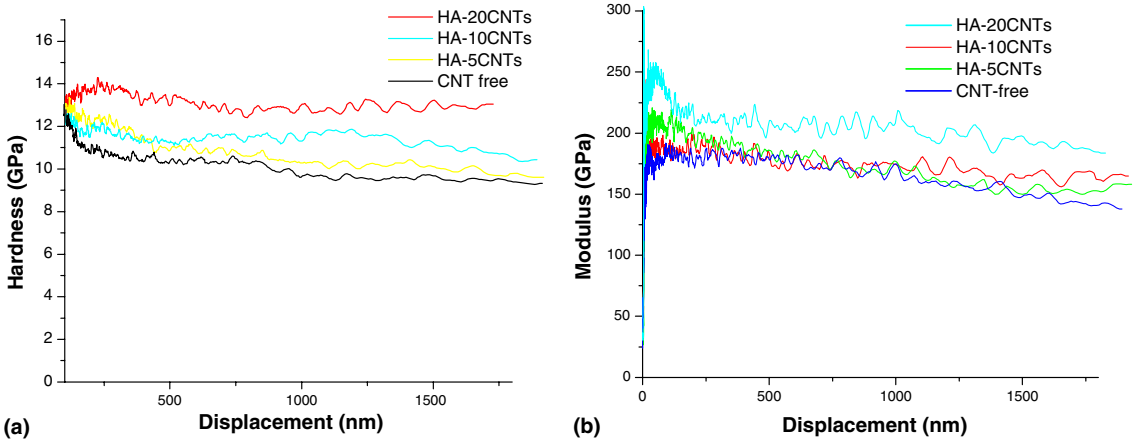

Fig. 7. Hardness (a) and elastic modulus (b) curves of as-alloyed coatings as a function of indentation depth.

Table 1
Values of Hardness and modulus of different laser surface alloyed coatings

	CNT-free coating	HA–5% CNTs coating	HA–10% CNTs coating	HA–20% CNTs coating
H (GPa)	9.347	10.216	11.873	13.342
E (GPa)	157.216	160.384	170.315	189.531

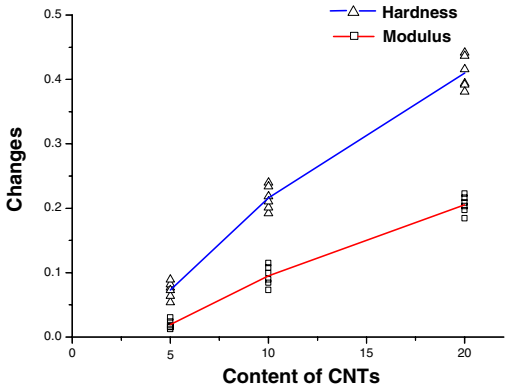

Fig. 8. Relative changes in hardness and modulus as a function of content of CNTs in starting precursor materials.

site coatings are indicated in Table 1. It shows that the hardness of these coatings increases with increasing of CNT content. It is well known that the carbon nanotube is one of the stiffest structures ever made [22] and, TiC also has higher hardness. Therefore, the residual CNTs and the in situ formation of TiC in the hydroxyapatite matrix, especially the residual CNTs, have an effective strengthening role in the composite coatings. Also, hardness and elastic modulus decrease with increasing the distance from the free surface of the coating respectively, the reason might be hardness and modulus elastic modulus are sensitive to the minor compositional disturbance and the compositional distribution along the coating depth is inhomogeneous in the laser-generated pool owing to the dilute effect of the substrate.

It has been reported that the value of elastic modulus of CNT is as high as approximately 1.8 TPa [22], which is much larger than that of hydroxyapatite. Generally, the addition of small content residual CNTs can cause the notable increase in the elastic modulus of these CNT reinforced hydroxyapatite coatings according to the simple rule of mixtures. The relative changes in hardness and modulus, $(Y - Y_H)/Y_H$ (Y_H is the parameters of the CNT-free coating, Y is the parameters of the

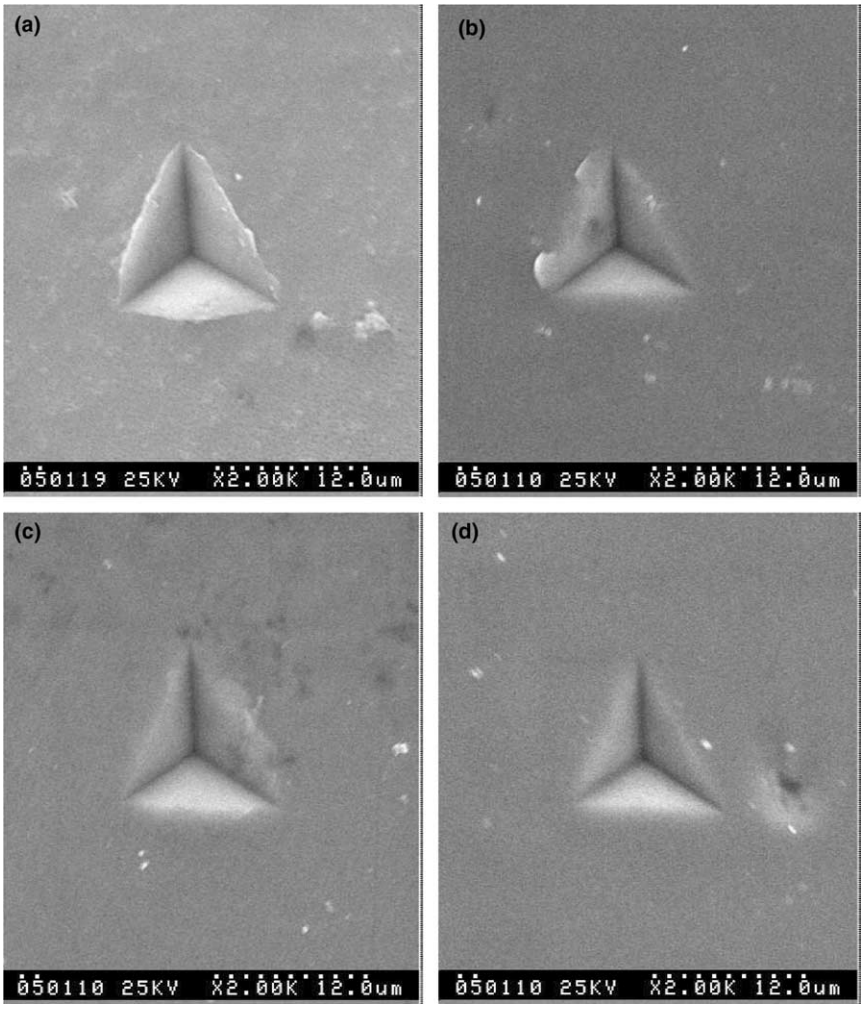

Fig. 9. SEM images showing the typical surface morphologies of indent marks for as-alloyed coatings with powder mixtures of CNT-free (a), HA–5% CNTs (b), HA–10% CNTs (c) and HA–20% CNTs (d).

CNT reinforced coatings) is shown in Fig. 8. It is clearly seen that the addition of CNTs has no strong effect on the value of modulus of these as-alloyed coating, but it has notable effect on the value of hardness of these composite coatings. The reason for this phenomenon might be that the multiwalled carbon nanotube usually has structural defects, which can result in the notable decrease of the value of the modulus [23]. It is worthy noting that the higher the value of the modulus of the biomaterial coating, the stronger the mismatch between coating and living bone tissues, due to the small value of the modulus of the bone tissues (20–30 GPa). Compared with the CNT-free hydroxyapatite coating, as the content of CNTs in the starting precursor materials increases, the remarkable increase in the hardness and slightly increase in the modulus of the CNT reinforced hydroxyapatite coating has a potential contribution toward improving the bone repair. As is known, the porosity of the material is an important factor for its mechanical behaviour. Therefore, how porosity changes with changing CNT content and effect of porosity on the mechanical properties of the laser surface alloyed CNT reinforced hydroxyapatite composite will be carried out under further investigation.

SEM images of the indent marks of different as-alloyed coatings are shown in Fig. 9, they represent overlapping layers of displaced material that flow upwards and way from the depth of the indent. With the increase in the content of CNTs, the significant decrease of the height of the pile-up is displayed, it illustrates that the higher content of CNTs, the higher resistance to plastic deformation, which is well agreement with the hardness measurement results.

4. Conclusions

In this paper, high-quality carbon nanotube (CNT) reinforced hydroxyapatite composite coatings have been successfully deposited on the surface of Ti–6Al–4V substrate using laser surface alloying. The bonding characteristics of the coating/substrate system are all of metallurgical fusion bonding. SEM images showed that the coatings have a rough surface with interlinking of pores, and TEM observation showed that a large amount of CNTs can be found with their original tubular morphology, even though some CNTs react with titanium element in the substrate during laser irradiation. The glassy phase was also found in the coating. Compared with the CNT-free hydroxyapatite coating, as the content of CNTs in precursor powders increases, the remarkable increase in the hardness and slightly increase in the modulus of the CNT reinforced hydroxyapatite coating has a potential contribution towards improving the bone repair. Therefore, CNT reinforced hydroxyapatite composite coating is a promising coating material for high-load-bearing metal implants.

Acknowledgement

The authors are grateful for the financial support from the Natural Science Foundation of China (Grant Nos. 50471088, 10372103 and 10432050) and China Postdoctoral Science Foundation (Grant No. 2004035073).

References

[1] Iijima S. Helical microtubules of graphitic carbon. Nature 1991;354:56–8.
[2] Baughman RH, Zakhidov AA, de Heer WA. Carbon nanotubes—the route toward applications. Science 2002;297:787–92.
[3] Thostenson ET, Ren Z, Chou TW. Advances in the science and technology of carbon nanotubes and their composites: a review. Compos Sci Technol 2001;61:1899–912.
[4] Dai H. Carbon nanotubes: opportunities and challenges. Surf Sci 2002;500:218–41.
[5] Lupo F, Kamalakaran R, Scheu C, Grobert N, Ruhle M. Microstructural investigations on zirconium oxide—carbon nanotube composites synthesized by hydrothermal crystallization. Carbon 2004;42:1995–9.
[6] Segger T, de la Fuente G, Maser WK, Benito AM, Callejas MA, Martinez MT. Evolution of multiwalled carbon-nanotube/SiO_2 composites via laser treatment. Nanotechnology 2003;14:184–7.
[7] Tadic D, Peters F, Epple M. Continuous synthesis of amorphous carbonated apatite. Biomaterials 2002;23:2553–9.
[8] Lynn AK, DuQuesnay DL. Hydroxyapatite-coated Ti–6Al–4V Part 1: the effect of coating thickness on mechanical fatigue behavior. Biomaterials 2002;23:1937–46.
[9] Khor KA, Fu L, Lim VJP, Cheang P. The effects of ZrO_2 on the phase compositions of plasma sprayed HA/YSZ composite coatings. Mater Sci Eng A 2000;276:160–6.
[10] Lim VJP, Khor KA, Fu L, Cheang P. Hydroxyapatite–zirconia composite coatings via the plasma spraying process. J Mater Process Technol 1999;89–90:491–6.
[11] Gu YW, Khor KA, Pan D, Cheang P. Activity of plasma sprayed yttria stabilized zirconia reinforced hydroxyapatite/Ti-6Al-4V composite coatings in simulated body fluid. Biomaterials 2004;25:3177–85.
[12] Ducheyne P, Beight J, Cuckler J, Evans B, Radin S. Effects of calcium phosphate coating characteristics on early post-operative bone tissue ingrowth. Biomaterials 1990;11:531–40.
[13] Kay JF. Calcium phosphate coatings for dental implants. Dent Clin North Am 1992;36:1–18.
[14] Zeng HT, Lacefield WR. XPS, EDX and FTIR analysis of pulsed laser deposited calcium phosphate bioceramic coatings: the effect of various process parameters. Biomaterials 2000;21:23–30.
[15] Cheng HM, editor. Synthesis, microstructure, properties and applications of carbon canotubes. Beijing: Chemistry Press; 2002. p. 4.
[16] Elghazal H, Lormand G, Hamel A, Girodin D, Vincent A. Microplasticity characteristics obtained through nano-indentation measurements: application to surface hardened steels. Mater Sci Eng A 2001;303:110–9.
[17] Oliver WC, Pharr GM. An improved technique for determining hardness and elastic modulus using load and displacement sensing indentation experiments. J Mater Res 1992;7:1564–83.

[18] Ji HX, Marquis PM. Effect of heat treatment on the microstructure of plas-sprayed hydroxyapatite coating. Biomaterials 1993;14:64–8.
[19] Yang CY, Wang BC, Chang E, Wu JD. The influence of plasma spraying parameters on the characteristics of hydroxyapatite coating: a quantitative study. J Mater Sci 1995;6:249–57.
[20] Ebbesen TW, Ajayan PM. Large-scale synthesis of carbon nanotubes. Nature 1992;358:220–2.
[21] Iijima S, Ichihashi T. Single-shell carbon nanotubes of 1-nm diameter. Nature 1993;364:603–5.
[22] Treacy MMJ, Ebbesen TW, Gibbson JM. Exceptionally high young' modulus observed for individual carbon nanotubes. Nature 1996;381:678–80.
[23] Gao RP, Wang ZL, Wang ZG, Heer WA, Dai LM, Gao M. Nanomechanics of individual carbon nanotubes from Pyrolytically Grown Arrays. Phys Rev Lett 2000;85:622–5.